# Highly Modular P−OP Ligands for Asymmetric Hydrogenation: Synthesis, Catalytic Activity, and Mechanism

**Héctor Fernández-Pérez,[a] Steven M. A. Donald,[a] Ian J. Munslow,[a] Jordi Benet-Buchholz,[a] Feliu Maseras,\*[a, b] and Anton Vidal-Ferran\*[a, c]**

**Abstract:** A library of enantiomerically pure P−OP ligands (phosphine–phosphite), straightforwardly available in two synthetic steps from enantiopure Sharpless epoxy ethers is reported. Both the alkyloxy and phosphite groups can be optimized for maximum enantioselectivity and catalytic activity. Their excellent performance in the Rh-catalyzed asymmetric hydrogenation of a wide variety of functionalized alkenes (26 examples) and modular design makes them attractive for future applications. The lead catalyst incorporates an (*S*)-BINOL-derived (BINOL=1,1′-bi-2-naphthol) phosphite group with computational studies revealing that this moiety has a dual effect on the behavior of our P−OP ligands. On one hand, the electronic properties of phosphite hinder the binding and reaction of the substrate in two out of the four possible manifolds. On the other hand, the steric effects of the BINOL allow for discrimination between the two remaining manifolds, thereby elucidating the high efficiency of these catalysts.

**Keywords:** asymmetric catalysis · catalyst tuning · hydrogenation · ligand design · P ligands

## Introduction

Over the past few decades, transition-metal-catalyzed transformations have become extremely powerful tools in asymmetric organic synthesis and many classes of chiral ligands have been developed, thereby providing highly efficient solutions for a growing number of asymmetric transformations.[1] Transition-metal-mediated asymmetric hydrogenation is a well-established and efficient methodology for the catalytic reduction of many prochiral substrates: alkenes, imines, and ketones.[2] From a practical perspective it has many advantages for the generation of new stereogenic centers, such as broad substrate scope, high reactivity and selectivity, as well as the minimal generation of waste.[3] There have been several significant breakthroughs in the field and now a myriad of chiral Ru-, Rh-, and Ir-coordination compounds (mostly phosphorus-containing derivatives) capable of mediating this transformation with very high enantioselectivities are known.[2,3] The development of commercial processes has rendered this transformation highly desirable to both academia and industry.[4]

Many groups, despite the remarkably advanced state of the field, are still actively researching new catalytic systems for challenging substrates, higher activity, and/or improved enantioselectivity. Research efforts have also been directed towards the development of chiral ligands with attractive industrial profiles, which means that they should induce high enantioselectivities, be easily prepared, and not be covered by current patents. Combinatorial and high-throughput synthetic strategies have led to the development of a number of highly efficient monodentate and bidentate phosphorus-containing ligands for asymmetric hydrogenation[5] that utilize either standard covalent[5c,6] chemistry or supramolecular interactions.[7] In a complementary way, ligand tuning in asymmetric catalysis has also allowed for the rapid development of efficient systems. When developing or improving a catalytic process by means of catalyst tuning, it is crucial to progressively move to a more efficient catalytic system accord-

[a] Dr. H. Fernández-Pérez, Dr. S. M. A. Donald, Dr. I. J. Munslow, J. Benet-Buchholz, Prof. F. Maseras, Prof. A. Vidal-Ferran
Institute of Chemical Research of Catalonia (ICIQ)
Avgda. Països Catalans 16, 43007 Tarragona (Spain)
Fax: (+34) 977920228
E-mail: fmaseras@iciq.es
avidal@iciq.es

[b] Prof. F. Maseras
Departament de Química, Universitat Autònoma de Barcelona
08193 Bellaterra, Catalonia (Spain)

[c] Prof. A. Vidal-Ferran
Catalan Institution for Research and Advanced Studies (ICREA)
Passeig Lluís Companys 23, 08010, Barcelona (Spain)

Supporting information for this article is available on the WWW under http://dx.doi.org/10.1002/chem.200902915.

ing to mechanistic and molecular-interaction principles. Ideally, the synthetic route should allow for simple modification of the steric and electronic properties of the molecular fragments (modules) within the ligand. If these modules are designed in such a way that they can influence the catalytic site, then a more efficient catalytic system (in terms of conversion and enantioselectivity) should become accessible by changing their steric and electronic properties. Indeed, the steric and electronic properties of modules could be considered as the "input parameters" in the optimization process.[8–10] Recently we described a new library of P−OP ligands derived from enantiopure epoxides (Scheme 1) and
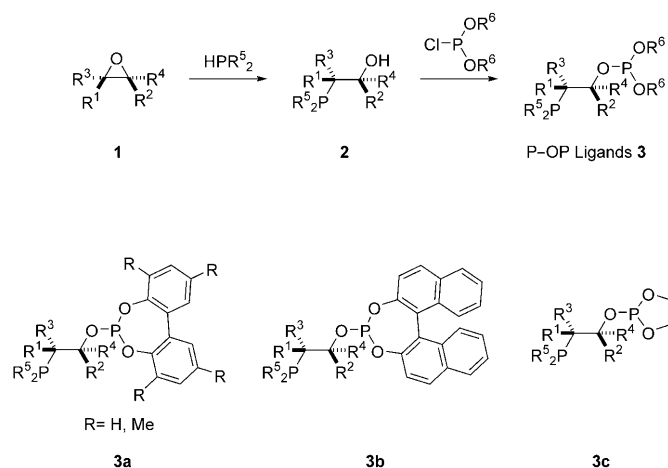


Scheme 1. New library of P−OP ligands derived from enantiopure epoxides.

their catalytic activity in Rh-mediated asymmetric hydrogenation.[9] Although P−OP ligands encompassing both diverse carbon backbones between the two phosphorus functionalities and stereogenic elements have been developed,[11–13] our phosphine–phosphites incorporate an understudied structural motif: two consecutive stereogenic centers between the two phosphorus functionalities. Herein we describe in full detail their modular synthesis, which contains a wide structural diversity that allows for simple catalyst optimization. The efficiency of these ligands in Rh-catalyzed asymmetric hydrogenation of functionalized alkenes (26 examples) is also discussed in this work.

Computational methods are becoming increasingly important in the field of asymmetric catalysis,[14] since they allow for the characterization of sophisticated reaction mechanisms and even the reproduction of experimental enantiomeric excesses.[15] Mechanistic knowledge on rhodium-catalyzed hydrogenation, specifically in the case of enamides, has benefited greatly from the contribution of computational chemistry. Following experimental proposals by Halpern et al.[16] and Brown,[2a,17] Landis et al.[18] were able to provide a detailed mechanistic picture for the process catalyzed by Rh(DuPHOS)$^+$, with initial approach of the substrate to the catalyst, oxidative addition of dihydrogen to rhodium, and

sequential migratory insertion of the olefinic carbon atoms into the metal–hydride bonds. The so-called *anti* lock-and-key effect, in which the lowest-energy pathway derives from the least stable catalyst–substrate adduct has also been satisfactorily explained. Complexes with Rh(BINAP)$^+$ (BINAP=2,2′-bis(diphenylphosphino)-1,1′-binaphthyl) have also been studied computationally and were shown to have a similar behavior.[19] Norrby, Wiest, and co-workers have used a quantum mechanics (QM)-guided method to satisfactorily reproduce the selectivity of a variety of $C_2$ catalysts with diphosphine ligands, including ligands such as BINAP and its derivatives, 4,12-bis(diphenylphosphino)-[2.2]paracyclophane (PHANEPHOS), (S)-(2-methoxyphenyl)-{2-[(2-methoxyphenyl)phenylphosphanyl]ethyl}phenylphosphane (DIPAMP), and others.[20] Calculations have also been performed that explain the experimentally proven[21] exceptions to lock-and-key behavior with monophosphite ligands[22] and the different mechanisms[2h,23,44] proposed by Gridnev et al., with initial formation of a dihydride species or alkene dissociation during the catalytic cycle.

In terms of the origins of enantioselection, computational studies have provided a quantitative base to the simple quadrant diagrams like that shown in Figure 1, initially proposed by Knowles.[24] For a $C_2$ catalyst like DuPHOS, two of the quadrants are blocked by steric effects and this leaves the olefin with only two low-energy directions of approach, both of which lead exclusively to the favored enantiomer. These quadrant diagrams represent of course a simplified view that is unable to explain all possible experimental situations, but it would be desirable to find an equivalent model for $C_1$ chelating ligands. In this work we also report a computational study of the asymmetric hydrogenation of acrylic acid derivatives mediated by our P−OP ligands to explain how these $C_1$ ligands are able to achieve comparable efficiency to the more usual $C_2$ diphosphines.
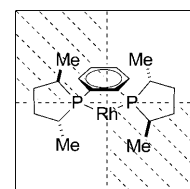


Figure 1. Quadrant diagram for DuPHOS. Sterically hindered quadrants are dashed.

## Results and Discussion

**Synthesis of phosphine–phosphite ligands**: In accordance with our goal of a highly modular synthetic methodology, we prepared a wide variety of phosphine–phosphite ligands **3** (11 examples). Our synthetic strategy was based on the use of enantiomerically pure epoxides as starting materials, from which our target ligands should be available in two well-precedented transformations: ring-opening of an epoxide with nucleophilic trivalent phosphorus derivatives followed by O-phosphorylation of the intermediate phosphino alcohols with trivalent phosphorus electrophiles (Scheme 1). The principles of the synthesis have been published in a previous communication.[9] We envisaged that this stepwise syn-

thetic route would allow for the preparation of our target modular P−OP ligands while permitting us 1) the incorporation of up to six molecular fragments, 2) control of the stereogenic centers between the P groups, and 3) modification of the steric and electronic properties of the two phosphorus functionalities.

The ring-opening of these Sharpless epoxy ethers proceeded smoothly at −30 °C to room temperature (63–83 % yield; Scheme 2). Single crystals of **5e** and **5f** suitable for X-ray diffraction were obtained,[25] which confirmed the regioselectivity of the ring opening (nucleophilic attack at the benzylic position) and an *anti* arrangement of the hydroxy and phosphino substituents in **5**, as expected for a stereospecific $S_N2$-like oxirane ring opening (inversion at the attacked carbon and retention at the other). Phosphine–phosphite ligands **6**, **7a–h**, and **8a,b** were all prepared following the same synthetic protocol (Scheme 2). Firstly, the free phosphino alcohols were obtained by decomplexation of the borane adducts **5a–f**, using 1,4-diazabicyclo[2.2.2]octane (DABCO) at 60 °C for diphenylphosphino-substituted compounds **5a–e** or diethylamine heated at reflux for the di-*tert*-butyl-substituted analogue **5f**. The phosphino alcohols were then derivatized in situ in the presence of an auxiliary base and the required chlorophosphite (Scheme 2).
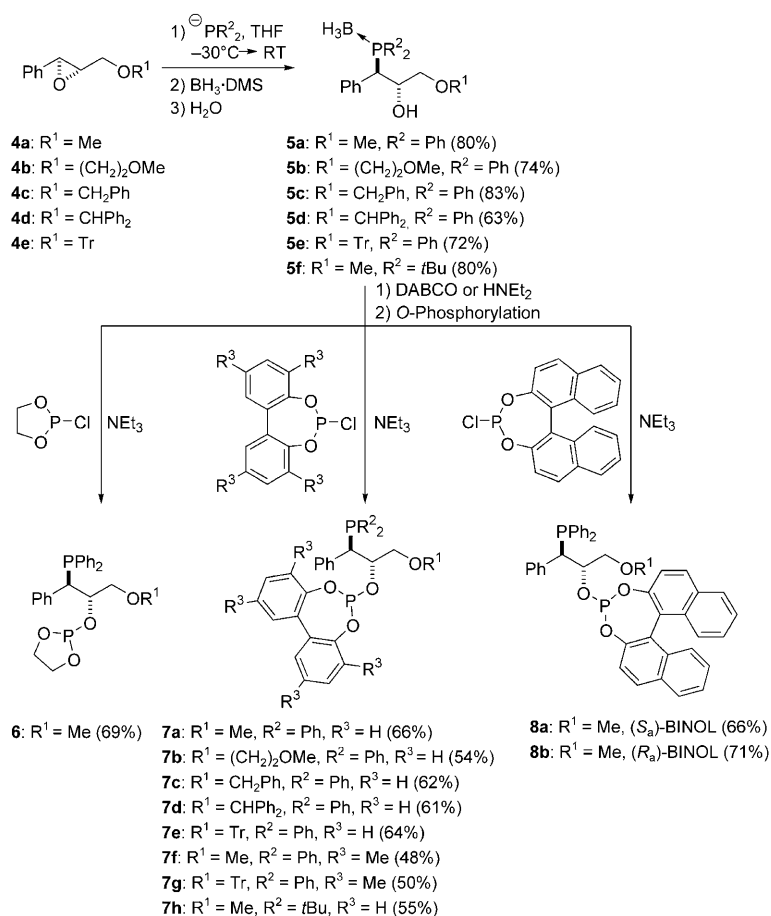
Phosphine–phosphites **7a–e** allow us to examine a wide range of steric bulk in the alkyloxy positions, thus encompassing methyl, methoxyethyl, benzyl, benzhydryl, and trityl groups, respectively,[26] whereas ligands **6**, **7a–e**, **7f,g**, and **8a,b** reflect differences in the phosphite fragment. In ligand **6**, which lacks biaryl groups, the two oxygen atoms are connected by an ethane bridge. Compounds **7a–e** and **7f,g** contain bisphenol or the more sterically demanding (tetramethyl)bisphenol group, both of which are able to interconvert between their conformers. It was reasoned that interconversion should facilitate adjustment of the catalyst to the steric requirements of a given transformation. Ligands **8a** and **8b** were designed to incorporate an additional stereogenic element: their phosphite fragments derived from ($R_a$)- or ($S_a$)-BINOL (BINOL = 1,1′-bi-2-naphthol). Lastly, compound **7h** differs in the phosphine fragment, in which the bulky and electron-rich di-*tert*-butylphosphino was used.[27]

**Synthesis of Rh$^I$ complexes**: To demonstrate the general ability of bidentate P−OP ligands to form stable, well-defined complexes with transition metals, we converted several of these into cationic rhodium(I) complexes following well-established procedures.[12p] These complexes were prepared in good yields by reacting stoichiometric amounts of the chiral phosphine–phosphite ligands and [Rh(nbd)$_2$]BF$_4$ (nbd = norbornadiene) in dichloromethane. As desired, the corresponding complexes [Rh(nbd)(**7a**)]BF$_4$ (**9**), [Rh(nbd)(**7h**)]BF$_4$ (**10**), and [Rh(nbd)(**8a**)]BF$_4$ (**11**) were obtained; see Scheme 3. The $^{31}$P{$^1$H} NMR spectra for **9–11** showed two sharp doublet of doublets, from the $^{31}$P,$^{103}$Rh, and $^{31}$P,$^{31}$P couplings (Table 1), as expected for 1:1 Rh/ligand complexes. Furthermore, single crystals of **9** and **10** suitable for X-ray diffraction were obtained, thereby unambiguously confirming a six-membered chelate coordination mode of the P−OP ligands to the Rh center.[25]

$^{31}$P NMR spectroscopic titration studies showed that the chiral Rh complexes generated in situ from [Rh(nbd)$_2$]BF$_4$ and the corresponding P−OP ligand were identical to the isolated examples at molar ratios of Rh/ligand ranging from 1:0.5 to 1:1.1.[28] Interestingly, new rhodium-containing species were formed when an excess of phos-



**4a**: R$^1$ = Me
**4b**: R$^1$ = (CH$_2$)$_2$OMe
**4c**: R$^1$ = CH$_2$Ph
**4d**: R$^1$ = CHPh$_2$
**4e**: R$^1$ = Tr

**5a**: R$^1$ = Me, R$^2$ = Ph (80%)
**5b**: R$^1$ = (CH$_2$)$_2$OMe, R$^2$ = Ph (74%)
**5c**: R$^1$ = CH$_2$Ph, R$^2$ = Ph (83%)
**5d**: R$^1$ = CHPh$_2$, R$^2$ = Ph (63%)
**5e**: R$^1$ = Tr, R$^2$ = Ph (72%)
**5f**: R$^1$ = Me, R$^2$ = *t*Bu (80%)

**6**: R$^1$ = Me (69%)

**7a**: R$^1$ = Me, R$^2$ = Ph, R$^3$ = H (66%)
**7b**: R$^1$ = (CH$_2$)$_2$OMe, R$^2$ = Ph, R$^3$ = H (54%)
**7c**: R$^1$ = CH$_2$Ph, R$^2$ = Ph, R$^3$ = H (62%)
**7d**: R$^1$ = CHPh$_2$, R$^2$ = Ph, R$^3$ = H (61%)
**7e**: R$^1$ = Tr, R$^2$ = Ph, R$^3$ = H (64%)
**7f**: R$^1$ = Me, R$^2$ = Ph, R$^3$ = Me (48%)
**7g**: R$^1$ = Tr, R$^2$ = Ph, R$^3$ = Me (50%)
**7h**: R$^1$ = Me, R$^2$ = *t*Bu, R$^3$ = H (55%)

**8a**: R$^1$ = Me, ($S_a$)-BINOL (66%)
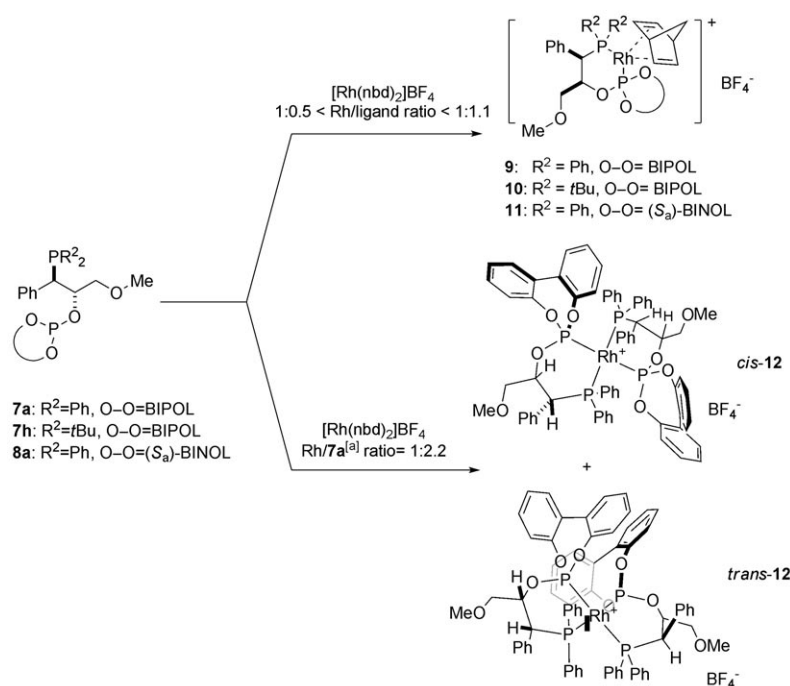**8b**: R$^1$ = Me, ($R_a$)-BINOL (71%)

Scheme 2. Synthesis of phosphine–phosphite ligands **6**, **7a–h**, and **8a** and **b** (overall yields are indicated in brackets; DMS = dimethyl sulfide).

Scheme 3. Rh-coordination studies on P–OP ligands **7** and **8**. [a] only studied for **7a**.

dium complexes generated in situ from 1.0 mol % of [Rh-(nbd)$_2$]BF$_4$ and a 10 mol % excess, with respect to Rh, of the P–OP ligand under 20 bar H$_2$. Although all ligands gave extremely high conversions in the reduction of **13** (see Table 2), enantioselectivities varied greatly. In the reduction of **13**, ligand **6**, which contained the least sterically demanding phosphite fragment, provided only moderate selectivities: 78 % *ee* (entry 1, Table 2). Ligand **7a**, which featured a bisphenol moiety, gave a higher enantioselectivity: 92 % *ee* (entry 2, Table 2). Better enantioselectivities (up to 98 % *ee*) were obtained for ligands **7a–e** when the hydrogenations were run at lower temperatures (entries 2 and 3, Table 2). We next

Table 1. $^{31}$P{$^1$H} NMR spectroscopic data for complexes [Rh(nbd)(P–OP)]BF$_4$ **9–11**.[a]

| Complex | P-O (phosphite moiety) | | | P-C (phosphine moiety) | | |
|---|---|---|---|---|---|---|
| | $\delta$ | $J$(P,Rh) | $J$(P,P) | $\delta$ | $J$(P,Rh) | $J$(P,P) |
| **9** | 135.7 | 266 | 66 | 30.2 | 146 | 66 |
| **10** | 138.6 | 277 | 55 | 65.1 | 139 | 55 |
| **11** | 138.9 | 268 | 65 | 35.2 | 144 | 65 |

[a] Chemical shifts ($\delta$) in ppm, coupling constants ($J$) in hertz.

phine–phosphite **7a** was used. These new rhodium-containing species, **12**, were prepared by reacting 1.0 equiv of [Rh-(nbd)$_2$]BF$_4$ with 2.2 equiv of phosphine–phosphite (48 % yield). $^{31}$P{$^1$H} and $^1$H NMR spectroscopic data revealed that the isolated rhodium complex was comprised of a mixture of *cis*-**12** and *trans*-**12** isomers in the ratio 1.3:1. In conclusion, an excess of phosphine–phosphite with respect to the rhodium precursor favors the formation of 2:1 chelates. Since 2:1 chelates of this kind were found to exhibit no catalytic activity in hydrogenations,[13q] the in situ formation of the rhodium precatalytic species demands careful control over the relative stoichiometry of [Rh(nbd)$_2$]BF$_4$ and P–OP ligand.

**Asymmetric hydrogenation**: With a highly modular synthetic methodology for the preparation of a wide variety of new ligands in hand, we set about evaluating their activity and selectivity in rhodium-mediated asymmetric hydrogenations. In the first set of experiments, we examined their use in the reduction of methyl (*Z*)-*N*-acetylaminocinnamate (**13**) as test substrate.[29] The reductions were performed using rho-

Table 2. Asymmetric hydrogenation of methyl (*Z*)-*N*-acetylaminocinnamate **13**.[a]
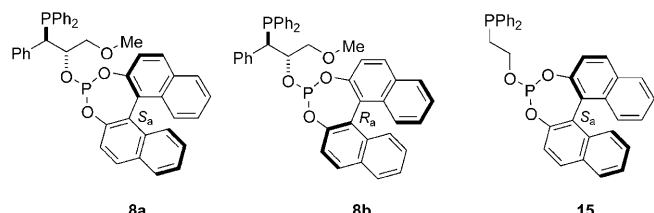


| Entry | Chiral ligand | $T$ [°C] | Solvent | Conversion [%][b] | *ee* [%][c] (configuration)[d] |
|---|---|---|---|---|---|
| 1 | **6** | RT | THF | >99 | 78 (*R*) |
| 2 | **7a** | RT | THF | >99 | 92 (*R*) |
| 3 | **7a** | −40 | THF | >99 | 98 (*R*) |
| 4 | **7b** | −40 | THF | >99 | 98 (*R*) |
| 5 | **7c** | −40 | THF | >99 | 97 (*R*) |
| 6 | **7d** | −40 | THF | 94 | 95 (*R*) |
| 7 | **7e** | −40 | THF | >99 | 92 (*R*) |
| 8 | **7h**[e] | RT | THF | >99 | 84 (*R*) |

[a] All reactions were carried out with a substrate/catalyst ratio of 100:1 for 12 h at 20 bar H$_2$ pressure and at the indicated temperature. [b] Conversion was determined by $^1$H NMR spectroscopy. [c] Enantiomeric excess was determined by HPLC. [d] The absolute configuration was assigned on the comparison with published data. [e] 1 mol % of [Rh(nbd)-(**7h**)]BF$_4$ (**10**) was used as the catalyst.

examined the effect of the R$^1$ group by systematically increasing its steric bulk on ligands **7a–e**: Me < (CH$_2$)$_2$OMe < CH$_2$Ph < CHPh$_2$ < CPh$_3$. A small negative effect on enantioselectivity (entries 3–7, Table 2) was observed upon increasing the size of the R$^1$ group. Ligand **7h** (R$^2_2$ = di-*tert*-butyl), which contained a bulkier phosphine moiety, gave slightly reduced *ee* values (entry 8, Table 2) than did ligand **7a** (R$^2_2$ = diphenyl; entry 2, Table 2).

Ligand **8a**, which contained an additional stereogenic element (a phosphite derived from ($S_a$)-BINOL), afforded excellent results with quantitative conversions and 99% *ee* for test substrate **13** (entry 1, Table 3).[29] Interestingly, while

Table 3. Contribution of the stereogenic centers in the ligand carbon backbone to the stereoselectivity in the asymmetric hydrogenation of **13**.[a]



| Entry | Substrate | Ligand | Reaction conditions | Conversion [%] | *ee* [%] (configuration) |
|---|---|---|---|---|---|
| 1 | **13** | **8a** | THF, RT | >99 | 99 (*R*) |
| 2 | **13** | **8b** | THF, RT | >99 | 84 (*S*) |
| 3 | **13** | **15** | THF, RT | >99 | 80 (*R*) |

[a] See Table 2 for details on the hydrogenation.

using its diastereomer **8b**, a phosphite unit derived from ($R_a$)-BINOL, the opposite absolute configuration of the hydrogenated product was obtained, though with lower enantioselectivity (cf. entry 2, Table 3). In an indication that the direction of stereodiscrimination is predominantly controlled by the binaphthyl group, **8a** contains the matched combination of the stereogenic centers in the carbon backbone between the two phosphorus functionalities and the stereogenic axis in the phosphite group.[30] The contribution of the stereogenic centers to stereoinduction was assessed by synthesizing ligand **15**, which contained an ethylene group between the phosphorus functionalities.[31] Interestingly, enantioselectivity obtained with ligand **15** was lower for test substrate **13**[29] than when compared to the one obtained using ligand **8a** (cf. entries 1 and 3 in Table 3). Hence, it suggests that the high selectivity is the result of a combined action between the chiral BINOL–phosphite moiety and ligand backbone chirality.

We also studied the influence of the rhodium precursor, with both the two commercially available precursors ([Rh-(nbd)₂]BF₄ and [Rh(cod)₂]BF₄) providing very similar conversions and enantioselectivities (entries 1 and 2, Table 4). These results are in agreement with literature reports,[32] which indicate that the presence of norbornadiene (nbd) or cyclooctadiene (cod) in the initial rhodium precursor only influences the transformation of the precatalyst into the catalytic species and has a much less pronounced effect on stereoselectivity. However, compared to the tetrafluoroborate counteranion, the bulkier hexafluoroantimoniate leads to reduced enantioselectivities (entry 3, Table 4). We also compared how the preparation of the precatalyst [Rh(nbd)-(**7a**)]BF₄ (i.e., preformed versus in situ preparation) affects the reaction. As mentioned in the previous section, a mixture of [Rh(nbd)₂]BF₄ with a 10% molar excess of the phos-

Table 4. Effect of the rhodium precursor on the asymmetric hydrogenation of methyl (*Z*)-*N*-acetylaminocinnamate.[a]

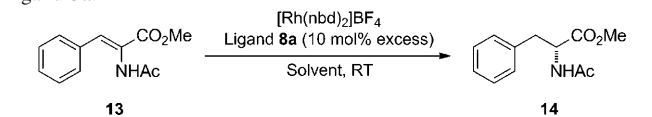| Entry | Catalyst[b] | Reaction conditions | Conversion [%] | *ee* [%] (configuration) |
|---|---|---|---|---|
| 1 | [Rh(nbd)₂]BF₄+**7a** | THF, RT | >99 | 92 (*R*) |
| 2 | [Rh(cod)₂]BF₄+**7a** | THF, RT | >99 | 91 (*R*) |
| 3 | [Rh(cod)₂]SbF₆+**7a** | CH₂Cl₂, RT | >99 | 79 (*R*) |
| 4 | [Rh(nbd)(**7a**)]BF₄ (**9**) | THF, RT | >99 | 92 (*R*) |

[a] See Table 2 for details on the hydrogenation. [b] 1 mol% of Rh precatalyst was used in all cases and 1.1 mol% of **7a** was used for entries 1, 2, and 3.

phine–phosphite affords the desired 1:1 chelate [Rh(nbd)-(**7a**)]BF₄ as the major rhodium-containing species.[28] As shown in Table 4, no differences in catalytic performance were observed between in situ preparation of the catalyst (entry 1, Table 4) versus preformed catalyst (entry 4, Table 4).

**Optimization**: We then investigated and optimized reaction conditions mediated by ligand **8a**. Initially we examined the optimal substrate/catalyst loadings in the reduction of **13**. Overnight reactions, at 20 bar H₂, with catalyst loadings as low as 0.04 mol% (substrate/catalyst ratio=2500:1) still gave quantitative conversions and up to 99% *ee* (entry 1, Table 5). However, no noticeable effects on enantioselectivity were observed upon changing the solvent or H₂ pressure with ligand **8a**, as shown in Table 5.

Table 5. Solvent and pressure dependency in the reduction of **13** with ligand **8a**.[a]



| Entry | Solvent | Rh precursor [mol%] | H₂ [bar] | Conversion [%] | *ee* [%] (configuration) |
|---|---|---|---|---|---|
| 1 | THF | 0.04 | 20 | >99 | 99 (*R*) |
| 2 | MeOH | 0.1 | 2 | >99 | 99 (*R*) |
| 3 | THF | 1 | 1 | 90 | 99 (*R*) |
| 4 | THF | 1 | 3 | >99 | 99 (*R*) |
| 5 | THF | 1 | 10 | >99 | 99 (*R*) |
| 6 | THF | 1 | 20 | >99 | 99 (*R*) |
| 7 | MeOH | 1 | 20 | >99 | 99 (*R*) |
| 8 | CH₂Cl₂ | 1 | 20 | >99 | 99 (*R*) |
| 9 | toluene | 1 | 20 | >99 | 99 (*R*) |
| 10 | THF | 1 | 80 | >99 | 98 (*R*) |

[a] See Table 2 for details on the hydrogenation.

In homogeneous catalysis there is a need for catalyst recycling and product separation, especially in the case of expensive catalysts that involve transition metals such as rhodium. We were very interested in investigating the product separation and the reuse of our catalytic system following the method of Börner et al., which involved the use of propylene carbonate as solvent.[33] Propylene carbonate has been shown to solubilize Ir- or Rh-containing catalytic systems

and has proven to be an ideal solvent for hydrogenation. If the hydrogenated compound is sufficiently soluble in nonpolar solvents such as alkanes, then the final products can be separated from the propylene carbonate solution by liquid–liquid extraction: the catalyst remains exclusively in the propylene carbonate phase, whereas the hydrogenation product can be extracted into the nonpolar phase.[33] To assess the recycling ability of rhodium complex [Rh(nbd)(8a)]BF$_4$, we used dimethyl itaconate **16x** as representative substrate for hydrogenation. Alkene **16x** was reduced in propylene carbonate under the standard hydrogenation conditions: in situ generation of the precatalyst (1.0 mol% [Rh(nbd)-(8a)]BF$_4$), room temperature, and 20 bar of hydrogen gas. After the required reaction time, the hydrogenated compound was extracted with cyclohexane. As reflected in Table 6, the catalyst can be reused up to four times with almost no change in catalytic activity (entries 2–5 in Table 6).

**Substrate scope**: Having obtained promising results from our initial ligand screening and from subsequent optimization of the reaction conditions, we then examined the efficiency of the best-performing ligand **8a** in hydrogenations of a structurally diverse array of substrates. The results of the corresponding hydrogenations are summarized in Table 7.

In general, regardless of the electronic or positional nature of the substituents on the aromatic ring, or whether the carboxyl group was an acid, the substrates were hydro-

Table 6. Recycling experiments of substrate **16x** with [Rh(nbd)-(**8a**)]BF$_4$.[a]



| Entry | Cycle[b] | Conversion [%] | ee [%] (configuration) |
|---|---|---|---|
| 1 | 1 | >99 | 99 (R) |
| 2 | 2 | >99 | 98 (R) |
| 3 | 3 | >99 | 97 (R) |
| 4 | 4 | >99 | 97 (R) |
| 5 | 5 | >99 | 96 (R) |

[a] See Table 2 for details on the hydrogenation. [b] The catalyst was reused after liquid–liquid extraction with cyclohexane. Every extraction allowed us to recover the hydrogenated product in 80% yield.

genated with high enantioselectivity (up to 99% ee) with **8a**. An important feature of the phosphine–phosphite ligands is their tolerance to a broad variety of amino-protecting groups (t-butyloxycarbonyl (Boc), benzyloxycarbonyl (Cbz), and 9-fluorenylmethoxycarbonyl (Fmoc): 7 examples), as demonstrated in the excellent selectivities observed, (entries 9, 10, 12, 14, and 17–19, Table 7).[34] Interestingly, in the reduction of alkene **16k** with an E configuration, low conversion, low enantioselectivity, and a reversal of the configuration of the hydrogenated product **17k** were observed (entry 11). Analogously, the E isomers of the Fmoc-containing substrates **16m** and **16o** could not be reduced, even at increased H$_2$ pressure (entries 13 and 15). Indeed, a very high Z selectivity was also observed in the reduction of **16p** (E/Z ratio 1:2.8). Ligand **8a** reduced only the Z isomer (56% ee, entry 16 in Table 7). This situation has been observed with other ligands.[34a] Certain ligands afford high enantioselectivity for aromatic dehydroamino acids, but not for the corresponding alkyl-substituted analogues.[35] We were pleased to discover that our catalytic system derived from **8a** afforded high enantioselectivity for the N-Boc-alkylamino acid substrate **16q** (entry 17). Lastly, concerning the preparation of enantiopure substituted alanines, (R)-N-Boc-3,5-difluorophenylalanine derivatives were obtained in high enantiomeric purity by hydrogenation of substrates **16r** and **16s**. These (R)-N-Boc-phenylalanine derivatives are key building blocks in
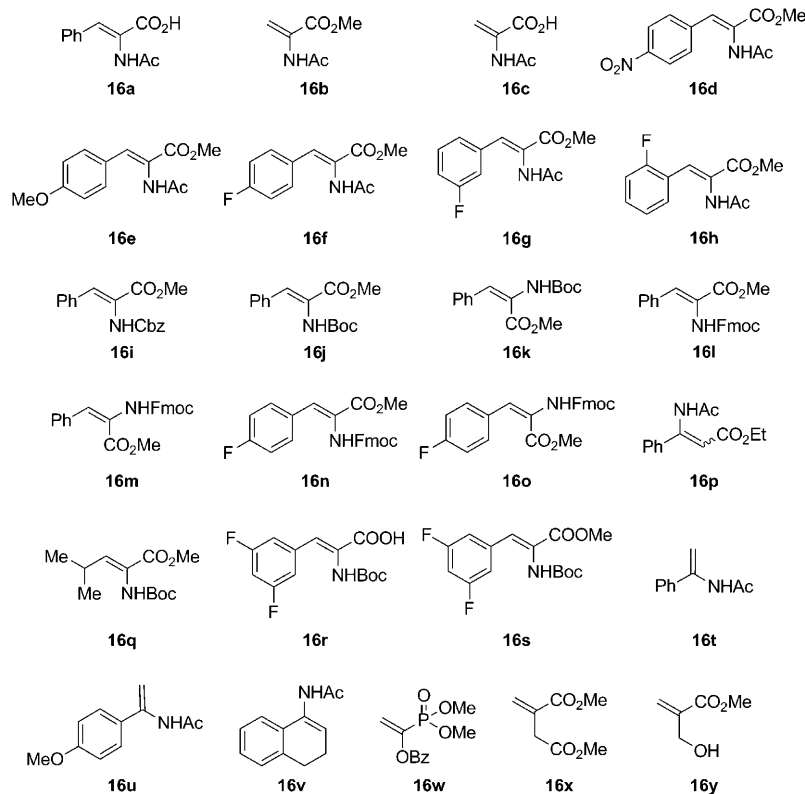
Table 7. Asymmetric hydrogenation of substrates **16** using ligand **8a**.[a]

| Entry | Substrate | Pressure [bar] | T [°C] | Solvent | Conversion [%][b] | ee [%][c] (configuration)[d] |
|---|---|---|---|---|---|---|
| 1 | **16a** | 20 | RT | THF | > 99 | 99 (R) |
| 2 | **16b** | 20 | RT | THF | > 99 | 99 (R) |
| 3 | **16c** | 20 | RT | THF | > 99 | 99 (R) |
| 4 | **16d** | 20 | RT | THF | > 99 | 99 (R) |
| 5 | **16e** | 20 | RT | THF | > 99 | 99 (R) |
| 6 | **16f** | 20 | RT | THF | > 99 | 99 (R) |
| 7 | **16g** | 20 | RT | THF | > 99 | 99 (R) |
| 8 | **16h** | 20 | RT | THF | > 99 | 99 (R) |
| 9 | **16i** | 20 | RT | THF | > 99 | 98 (R) |
| 10 | **16j** | 20 | RT | THF | > 99 | 96 (R) |
| 11 | **16k** | 20 | RT | THF | 13 | 28 (S) |
| 12 | **16l** | 40 | RT | THF | > 99 | 98 (R) |
| 13 | **16m** | 80 | RT | THF | 0 | n.a.[e] |
| 14 | **16n** | 40 | RT | THF | 94 | 97 (R)[g] |
| 15 | **16o** | 80 | RT | THF | 0 | n.a.[e] |
| 16 | **16p**[f] | 20 | RT | THF | 74 | 56 (R) |
| 17 | **16q** | 40 | RT | THF | 70 | 92 (R) |
| 18 | **16r** | 20 | RT | THF | > 99 | 96 (R) |
| 19 | **16s** | 20 | RT | THF | > 99 | 96 (R) |
| 20 | **16t** | 20 | RT | THF | > 99 | 98(R) |
| 21 | **16u** | 20 | RT | THF | > 99 | 97 (R) |
| 22 | **16v** | 20 | RT | THF | > 99 | 57 (R) |
| 23 | **16w** | 20 | RT | CH₂Cl₂ | > 99 | 92 (S) |
| 24 | **16x** | 20 | RT | CH₂Cl₂ | > 99 | 99 (R) |
| 25 | **16y** | 20 | 0 | THF | > 99 | 95 (S) |

[a] All reactions were carried out with a substrate/catalyst ratio of 100:1 at room temperature for 12 h at the $H_2$ pressure indicated. [b–d] Conversion, enantiomeric excess, and absolute configuration were determined as indicated in Table 2. [e] Not analyzed. [f] Starting material *E/Z* ratio 1:2.8. [g] Unreported optical rotation or chromatographic elution order; absolute configuration was tentatively assigned to be *R* by analogy based on the stereochemical outcome for **13**, **16a**, **16d–j**, and **16l**.

Table 8. Comparison of the catalytic activity obtained with our ligand **8a** to those obtained with ligands **19–21** in rhodium-catalyzed asymmetric hydrogenation.
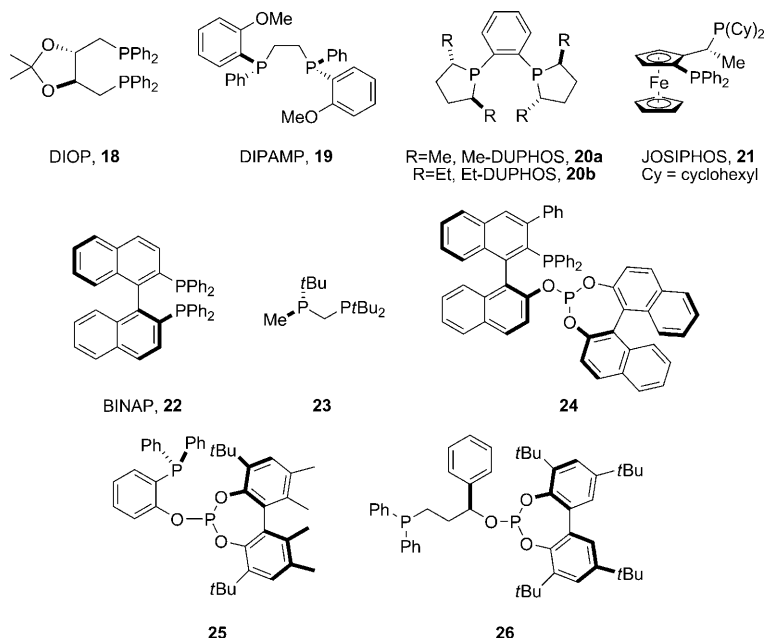
| Entry | Ligand | Substrate-to-catalyst ratio | Substrate | H₂ [bar] | Solvent | TOF [h⁻¹] |
|---|---|---|---|---|---|---|
| 1 | **8a** | 1000 | **13** | 2 | MeOH | 1200 |
| 2 | **8a** | 1000 | **13** | 20 | THF | 1600 |
| 3 | **19** | 1000 | **13** | 3 | MeOH | 440[34a] |
| 4 | **20a** | 10000 | **13** | 3 | MeOH | 4800[34a] |
| 5 | **21** | 5000 | **13** | 3 | MeOH | 960[34a] |

enzymatic processes, degradation of homoallylic acetates, additions to ketenes, or aldol reactions.[38b–c]

One can see from Table 8 and Table 9 that ligand **8a** compares very favorably to what are often called milestone ligands in rhodium-catalyzed asymmetric hydrogenations (i.e., DuPHOS, JOSIPHOS, etc.) as well as other related ligands in Rh-mediated hydrogenations of structurally diverse alkenes.

## Computational study of the mechanism

*Four possible manifolds*: To shed light on the correlation between enantioselection and the features of the P−OP ligands, we present here a theoretical investigation into the reactivity of our lead catalyst **8a** (derived from $(S_a)$-BINOL), and its $(R_a)$-BINOL-derived diastereomer **8b** with methyl N-acetylaminoacrylate (**16b**). This is the system that gives the higher enantiomeric excess, and an understanding

the preparation of novel renin inhibitors for treating hypertension.[36]

High enantioselectivities were obtained for α-aryl enamides **16t** and **16u** (entries 20 and 21), whereas only moderate enantioselectivity was observed for the challenging α-tetralone-derived enamide **16v** (57 % ee, entry 22).[37] High enantioselectivity was also obtained for the enol ester phosphonate **16w** (entry 23). Itaconate derivatives are another class of compounds that yield interesting enantiopure derivatives upon asymmetric hydrogenation. Excellent enantioselectivities were also obtained in the hydrogenation of dimethyl itaconate **16x** (99 % ee, entry 24) and for the related Roche ester[38] **16y** (95 % ee,[39] entry 25). This compound is of significant industrial interest, and asymmetric hydrogenation provides a more atom-economical route than



DIOP, **18**    DIPAMP, **19**    R=Me, Me-DUPHOS, **20a** / R=Et, Et-DUPHOS, **20b**    JOSIPHOS, **21** / Cy = cyclohexyl

BINAP, **22**    **23**    **24**

**25**    **26**

of this system can help to understand the behavior of catalysts containing $C_1$ ligands, thereby aiding in the design of future catalysts.

Table 9. Comparison of the enantioselectivities obtained with our ligand **8a** to those obtained with ligands **18–26** in rhodium-catalyzed asymmetric hydrogenation of various alkenes.

| | Ligands | | | | | | | | | |
| | **18** | **19** | **20b** | **21** | **22** | **23** | **24** | **25** | **26** | **8a** |
|---|---|---|---|---|---|---|---|---|---|---|
| **16a** | 72 (R)[40] | 94 (S)[41] | – | 84 (S)[42] | 96 (R)[43][c] | >99 (R)[44] | 99 (S)[13i] | – | – | 99 (R)[45] |
| **13** | 68 (R)[46] | 96 (S)[41] | 99 (S)[47] | 96 (S)[42] | 93 (R)[43][c] | >99 (R)[44] | >99 (S)[13i] | >99 (R)[13e] | 97 (R)[12p] | 99 (R)[45] |
| **16c** | 73 (R)[40] | – | – | – | 98 (R)[43][c] | >99 (R)[44] | – | – | – | 99 (R)[45] |
| **16b** | – | – | >99 (S)[47] | 88 (S)[42] | 21 (R)[48] | >99 (R)[44] | >99 (S)[13i] | – | 99 (R)[12p] | 99 (R)[45] |
| **16p**[a] | 17[49] | 68[49] | 87[49] | – | – | – | – | – | – | 57 (R)[45] |
| **16t** | 53 (S)[50] | – | 95 (S)[51][b] | – | 11 (R)[48] | 98 (R)[44] | – | – | – | 98 (R)[45] |
| **16x** | 25 (R)[52] | 88 (R)[53] | 97 (R)[54][d] | 98 (S)[42] | 94 (S)[55] | 98 (S)[44] | – | >99 (S)[13e] | – | 99 (R)[45] |

[a] *ee* values for compound (Z)-**16p** and its methyl-substituted analogue. [b] Compound **16t** was reduced using (S,S)-Me-DUPHOS **20a**. [c] *ee* values correspond to the hydrogenation of the *N*-benzoyl-protected derivatives rather than the *N*-acetyl ones. [d] *ee* values for itaconic acid instead of dimethyl itaconate.

In contrast with the systems studied in the majority of theoretical investigations on asymmetric hydrogenation to date, the P–OP ligands **8a** and **8b** are not $C_2$ symmetric.[56] With $C_2$ symmetric ligands, there are only two distinct modes of binding the chelating substrate to the catalyst. These adducts have traditionally been labeled as **pro-R** and **pro-S** (Scheme 4) because of the prochiral nature of the ad-
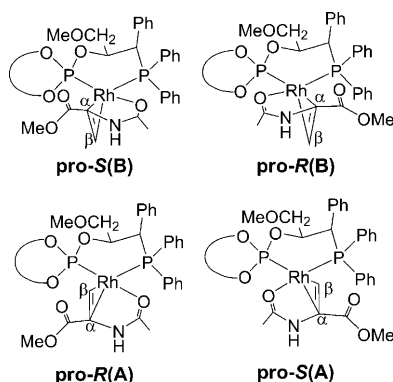


Scheme 4. The four possible binding modes for the substrate with the **8a**- and **8b**-ligated catalysts.

ducts, whereby dihydrogen will be added across the olefin, thus forming new carbon–hydrogen bonds from the side of the metal during the stereospecific catalytic process. For $C_1$ ligands such as the P–OP ones considered here, the equivalence between the two available rhodium binding sites is lost, and there are four possible binding modes in the catalyst–substrate adduct complexes, as shown in Scheme 4. We have used the arbitrary labels **A** and **B** for the additional source of configurational complexity, and as a result there are four different reaction manifolds to be considered: **R(A)**, **R(B)**, **S(A)**, and **S(B)**.

The nonsymmetrical nature of the catalyst also has important implications for the methodology applied in this computational investigation, given that the relative energies of each manifold will be affected not only by steric bulk of the ligand but also the electronic effect of the different phosphorus donor (P donor) atoms. We recently reported our density functional theory (DFT) and DFT/molecular me-

chanics (MM) investigations into the enantioselection in our first generation P–OP ligand (a phosphine–phosphinite), which proved that a full DFT description of the systems was essential to capture the full steric and electronic complexity of the system.[57] In addition, the highly flexible nature of the catalyst, with a six-membered backbone and free-rotating phosphine phenyl (P-phenyl) groups, requires a systematic conformational analysis. Details of the applied methodology are supplied in the Supporting Information.

*Identification of the rate-determining step*: The usual approach for computational studies on enantioselective catalysis is to focus on the single key step of the catalytic cycle and compare the energy of this transition state for the different paths leading to the *R* and *S* products.[15] The mechanism for rhodium-catalyzed hydrogenation of enamides is complex but, luckily, it has been systematically explored by a number of research groups. The key series of articles by Halpern et al.,[16] Brown,[2a,17] and Landis et al.[18] have resulted in the generally accepted "unsaturated" mechanism shown in Scheme 5. The mechanism consists of the following steps: 1) coordination of the substrate to the catalyst to form an adduct (**pro-R**, **pro-S**); 2) addition of dihydrogen to the catalyst–substrate adduct to form a 5-coordinate dihydrogen intermediate (**MolH₂**); 3) oxidative addition of dihydrogen to give the dihydride intermediate (**DIHY**); 4) migratory insertion of the β carbon of the olefin into a Rh–H bond to form an alkyl hydride complex with a C–H···Rh agostic bond (**ALHYag**); 5) breaking of the agostic bond to give a 5-coordinate alkyl hydride (**ALHY**); and 6) C–H reductive elimination to form the product, bound to the metal by the two carbonyl oxygen atoms (**Prod**). Previous computational studies have shown that the approach of dihydrogen to the catalyst–substrate adduct takes place in a direction parallel to the P–Rh–olefin bond, and that, for substrates similar to the one considered here, the first hydride addition is made to the β carbon of the substrate, as shown in Scheme 5.

In general, theoretical studies on hydrogenation observe competition between oxidative addition and migratory insertion as possible rate-determining steps.[20] We confirmed this observation by studying the energy profile of the full catalytic cycle in the reaction catalyzed by our first-generation
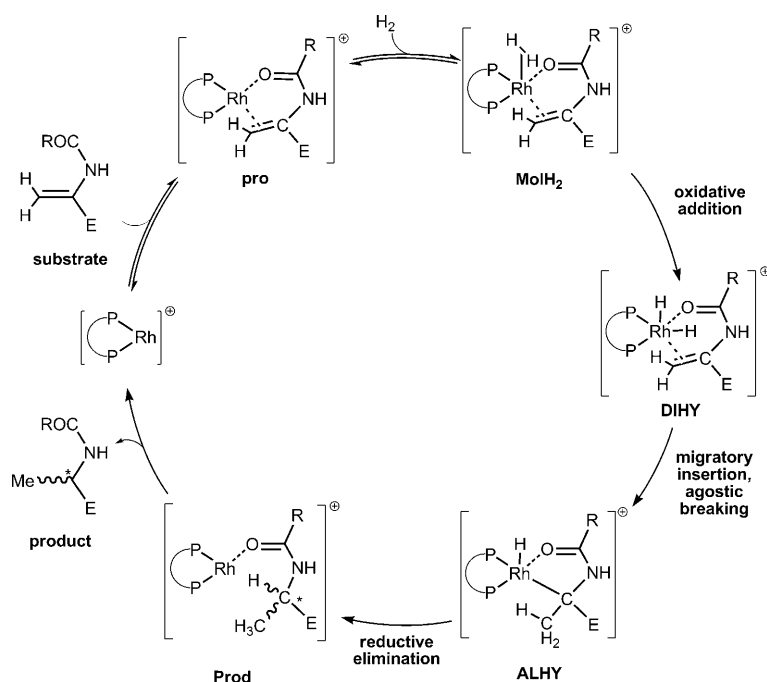
Scheme 5. The more common mechanism for asymmetric hydrogenation.

P–OP (phosphine–phosphinite) ligand.[57] The profile for one of the manifolds is presented in Figure 2. It shows that the highest energy corresponds to the transition state for oxidative addition, followed by that for migratory insertion.
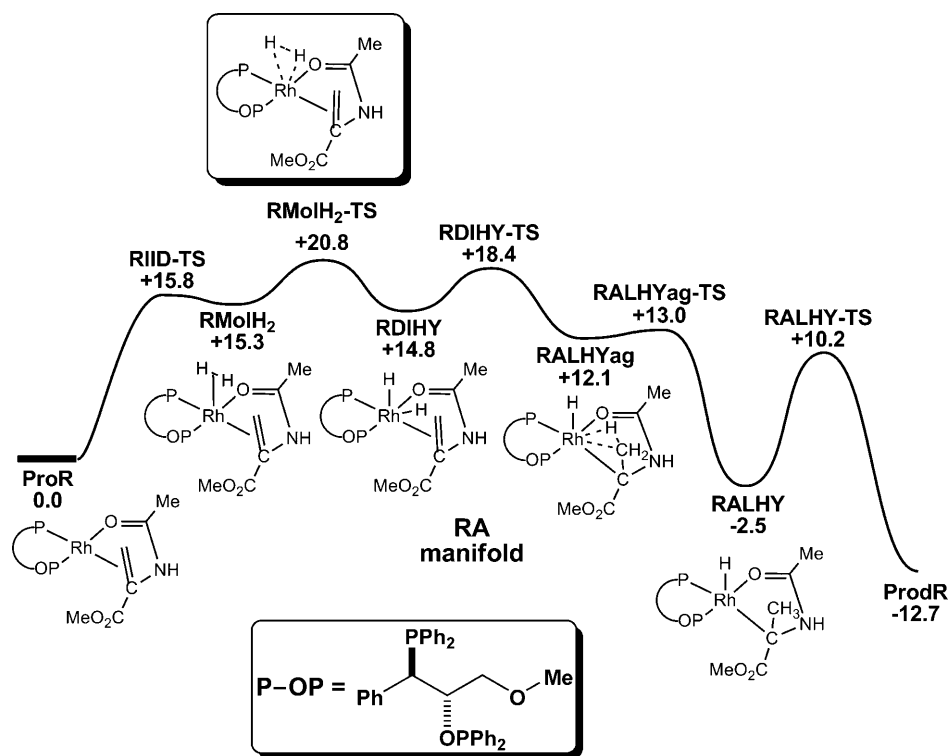
Oxidative addition has the highest energy for all cases we have tested, both on this phosphine–phosphinite system and the BINOL-derived systems **8a** and **8b**. The migratory insertion transition state has been checked in every single case, but it has always been found to be lower in energy, although in the more electron-rich **8a** and **8b** ligands, it is lower by less than 1 kcal mol$^{-1}$ compared to 1–3 kcal mol$^{-1}$ in the phosphine–phosphinite ligand (see the Supporting Information). Thus our calculations of the enantiomeric excess are based on structures obtained after a detailed conformational analysis of the oxidative addition transition states.

The alternative "dihydride" mechanism, in which dihydrogen oxidative addition occurs prior to substrate coordination, which has been observed under nonturnover conditions by Gridnev and co-workers[2h, 23, 44] seems limited to specific cases, usually involving highly electron-rich alkyl-phosphines, and thus is not related to the current case.

*Origin of enantioselectivity in the hydrogenation with (S$_a$)-BINOL-derived ligand 8a:* Having already determined that oxidative addition is rate determining in all four manifolds, we carried out full conformational assessment of the oxidative addition transition state (OATS) structures, the lowest energies of which are shown in Figure 3. Selected geometrical parameters are collected in Table 10. In calculating the enantiomeric excess for this catalyst, we include all possible conformations of all four manifolds for a more accurate result, and yield an *ee* value of 90% (*R*) (cf. 99% (*R*) experimentally). The experimental behavior is thus reproduced, and we can proceed to analyze its origin.

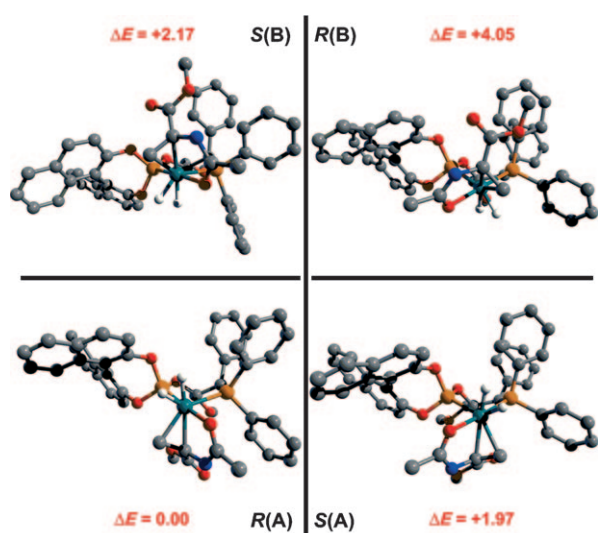The OATS structures feature the expected pseudo trigonal bipyramidal geometry, with



Figure 2. Free-energy profile (in kcal mol$^{-1}$) for one manifold of the complete catalytic cycle with the first-generation P–OP ligand.

Figure 3. Computed structures of the lowest-energy oxidative addition transition states (OATS) (relative free energies in kcal mol$^{-1}$) for ligand **8a**.

Table 10. Selected geometric parameters [Å] for the lowest-energy OATS structures in each manifold for ligand **8a**.

| OATS | 8a-*R*(A) | 8a-*S*(B) | 8a-*R*(B) | 8a-*S*(A) |
|---|---|---|---|---|
| H–H | 1.20 | 1.25 | 1.31 | 1.21 |
| Rh–C$_\alpha$ | 2.27 | 2.29 | 2.30 | 2.29 |
| Rh–C$_\beta$ | 2.18 | 2.17 | 2.18 | 2.20 |
| C$_\alpha$–C$_\beta$ | 1.42 | 1.42 | 1.41 | 1.41 |
| Rh–O | 2.14 | 2.16 | 2.15 | 2.15 |
| Rh–PO | 2.24 | 2.25 | 2.40 | 2.38 |
| Rh–PC | 2.51 | 2.50 | 2.34 | 2.34 |

both the olefin and the dihydrogen lying in the trigonal plane. The M–P bond length in the trigonal plane lengthens significantly (by up to 0.11 Å) from the corresponding adduct structures. This is due to the partially antibonding character of the equatorial positions in d$^8$ ML$_5$ complexes.[58] The key distances in the coordination sphere of rhodium (Table 10) are similar for all four manifolds, with the notable exception of the Rh–P distances. In this case, two blocks are clearly defined. For the **S(B)** and **R(A)** transition states, there are short Rh–PO (PO = phosphite side phosphorus) distances of 2.25 and 2.24 Å, respectively; and long Rh–PC (PC = phosphine side phosphorus) distances of 2.50 and 2.51 Å, respectively. For the **R(B)** and **S(A)** transition states, the distances are more similar and the order is inverted, 2.40

and 2.38 Å, respectively, for Rh–PO and 2.34 and 2.34 Å, respectively, for Rh–PC. This disparity in distances had been already observed to a smaller degree in our previous study on the phosphine–phosphinite ligand,[57] and points to an important characteristic of the system. The presence of oxygen substituents in the phosphite makes it a stronger σ donor than the phosphine, and it will thus prefer not to occupy a site in the equatorial plane, in which the antibonding character will result in Rh–P bond lengthening. For the **S(B)** and **R(A)** manifolds, the Rh–PO distances are shorter and thus electronically favored. For these same manifolds, the weaker Rh–PC bonds become as long as 2.51 Å. From an energetical point of view, this is the optimal situation, and as a result, the **S(B)** and **R(A)** manifolds are favored with respect to the **R(B)** and **S(A)** ones, in which the Rh–PO distances are up to 0.16 Å longer. This is reflected in the relative energies of the **R(A)**, **S(B)**, **S(A)**, and **R(B)** manifolds (0.0, 2.17 vs. 1.97, 4.05 kcal mol$^{-1}$, respectively). The electronic asymmetry on the P–OP ligand thus establishes a discrimination between the manifolds that was absent in the $C_{2v}$ ligands. This can be visualized in a quadrant diagram (Figure 4) by saying that the two right-hand sites are electronically disfavored with respect to placement of the C$_\alpha$ and C$_\beta$ olefin carbon atoms of the substrate.

The difference within each of the two pairs of manifolds with electronically similar properties is associated to steric effects. The accepted view[18] (Scheme 4) for the steric requirements of this type of enamide substrates is that, in the transition state, the steric hindrance appears in the quadrant originally occupied by the C$_\alpha$ olefin carbon. For the electronically favored pair of manifolds **S(B)** and **R(A)**, the olefin is bound *cis* to the phosphite donor containing the BINOL. In the case of BINOL, the steric hindrance is clearly associated with the quadrant in which a naphthyl group points towards the substrate. For ligand **8a**, this is the upper-left quadrant in the orientation shown in Figure 4. In the transition state of manifold **R(A)**, C$_\alpha$ is in the lower-left
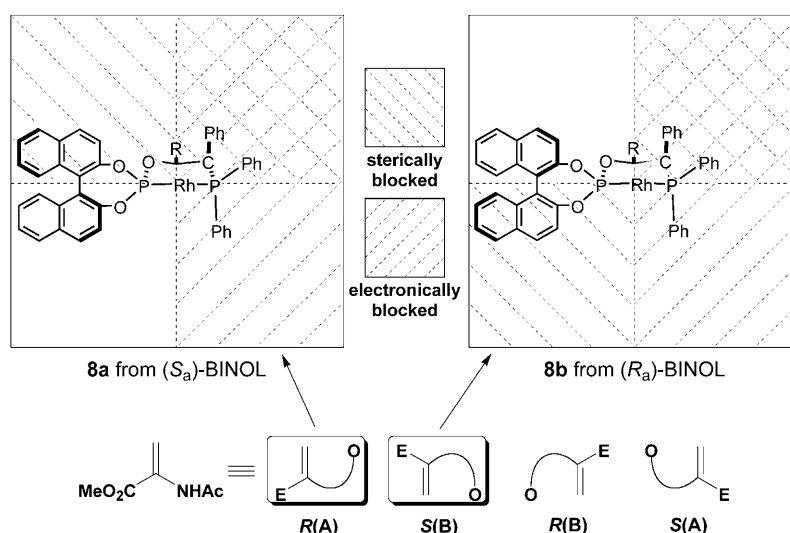


Figure 4. Quadrant representation for possible substrate orientations in the OATS with ligands **8a** and **8b**.

quadrant, far from the steric congestion of BINOL, and as a result this is the most favored manifold. For manifold **S(B)**, the steric congestion increases the energy by 2.17 kcal mol$^{-1}$. The difference in distances between olefin and naphthyl atoms is clear in both cases. The shortest H−H and H−C distances for sterically congested **S(B)** are 2.247 and 2.526 Å, respectively, whereas none of these distances are below 5 Å for the most stable **R(A)** transition state. The comparison for the electronically disfavored pair of manifolds **R(B)** and **S(A)** is also straightforward. The highest energy (by 2.08 kcal mol$^{-1}$) corresponds to the **R(B)** manifold because of the presence of the backbone phenyl, P-phenyl groups, and the α-ester substituent in the same quadrant.

In the discussion above, we have shown that enantioselection in the P−OP catalysts is a fine balance of electronic and steric effects. Primarily, the strong electronic effect of the phosphite donor results in almost complete blocking of product formation through the two manifolds with the olefin *trans* to phosphite (namely, **R(B)** and **S(A)**). The phenyl group in the backbone provides additional steric blocking to the **R(B)** manifold. The principal steric director in our P−OP catalysts is clearly the BINOL, which directly affects the favorability of the **R(A)** and **S(B)** manifolds.

We note finally that the mechanism follows *anti* lock-and-key behavior in this system. The most stable adduct (see the Supporting Information) is in the **S(B)** manifold, but product formation proceeds by means of the **R(A)** manifold.

*Origin of enantioselectivity in the hydrogenation with (R$_a$)-BINOL-derived ligand 8 b*: We followed the same procedure for ligand **8b** as in **8a**, with the lowest-energy structures for the OATS structures and selected geometrical parameters presented in the Supporting Information. As for **8a**, we included all possible conformations of all four manifolds for a more accurate result of the enantiomeric excess, by which we obtained an *ee* value of 95% (*S*) (cf. 88% (*S*) experimentally).

The qualitative picture closely follows the lines discussed above for **8a**. Manifolds **R(B)** and **S(A)** are disfavored by the electronic effects of the phosphorus donors, reflected in the different Rh−PO and Rh−PC distances. Manifold **R(B)** is further disfavored due to extreme steric crowding in the upper-right quadrant. Comparing the **R(A)** and **S(B)** manifolds, there is very little difference in the key metal geometry and metal–ligand parameters. Between these two favored manifolds, the difference is in the steric interactions. There is a repulsion present between the α-ester substituent and BINOL in the **R(A)** OATS, which is absent in the **S(B)** OATS and thus the reaction proceeds to product through **S(B)**.

Again, the mechanism follows *anti* lock-and-key behavior, in which the major product forms by means of the **S(B)** adduct, and not the favored **R(A)** adduct (see the Supporting Information for details on the adducts). The results for the P−OP systems with the **8a** and **8b** ligands are summarized in the quadrant diagram in Figure 4. The two right-hand quadrants are always disfavored by the electronic ef-

fects of BINOL, whereas one of the left-hand quadrants is blocked by the steric effects of BINOL. The sterically blocked quadrant depends on the stereochemistry of BINOL, which in this way decides the selectivity in the product. The quadrant diagram in Figure 4 smoothly integrates our current results on a $C_1$ diphosphine with well-established concepts for $C_2$ diphosphines (Figure 1), and points to a behavior that can be general for efficient $C_1$ ligands.

The computed results are in qualitative (and within 10% *ee* of quantitative) agreement with experimental results, but do not quite match the relative magnitudes of the observed enantioselection in each ligand, as we predict ligand **8b** (95% *ee* of *S* product) to be more effective than **8a** (90% *ee* of *R* product) and the experiment shows the opposite trend (88% *ee* of *S* vs. 99% *ee* of *R*). There is some kind of communication between the left and right quadrants of the system (matched vs. mismatched effect) that our model is unable to capture properly. However, the discrimination between 90 and 95% *ee* would require sub-kcal mol$^{-1}$ accuracies that should not be expected from our DFT method, especially taking into account that a balance between electronic and steric effects seems to be present in this case. At any rate, the current results provide a solid base for the explanation of the observed selectivities and provide a simple interpretation for the behavior of catalysts with phosphine–phosphite ligands.

## Conclusion

Chiral phosphine–phosphite ligands **6**, **7a–h**, and **8a,b**, easily derived from Sharpless epoxy ethers, have proven to be highly efficient ligands in the Rh-catalyzed reduction of a wide variety of functionalized alkenes (26 examples). In particular, the "lead" ligand of the series (**8a**) has been shown to have outstanding catalytic properties in this transformation and is able to tolerate a broad range of carbamate-type amino-protecting groups (Boc, Cbz, and Fmoc). The presence of the BINOL-derived phosphite group has thus a dual effect on the behavior of these $C_1$ ligands. On one hand, the electronic properties of phosphite hinder binding of the substrate in two out of the four possible manifolds, whereas on the other hand, its steric effects allow for the discrimination between the two remaining manifolds, thereby explaining the high efficiency of these catalysts.

The strategy described in this paper to discover new chiral catalysts—the tuning of the performance of the catalyst by modifying the steric and electronic properties of the molecular fragments or modules—is based on a correct hypothesis. The results described show that the different parts of a given chiral catalyst can be optimized separately, so that it is possible to achieve high levels of enantioselectivity even when starting from an initially mediocre ligand. Future work is in progress, applying these ligands towards new asymmetric reactions, such as allylic substitutions or in hy-

drogenations of challenging substrate classes (containing C=N and unfunctionalized C=C bonds).

## Acknowledgements

[1] *Comprehensive Asymmetric Catalysis, Vol. I–III* (Eds.: E. N. Jacobsen, A. Pfaltz, H. Yamamoto), Springer, Heidelberg, **1999**.

[2] a) J. M. Brown in *Comprehensive Asymmetric Catalysis, Vol. I* (Eds.: E. N. Jacobsen, A. Pfaltz, H. Yamamoto), Springer, Heidelberg, **1999**, p. 122; b) R. L. Halterman in *Comprehensive Asymmetric Catalysis, Vol. I* (Eds.: E. N. Jacobsen, A. Pfaltz, H. Yamamoto), Springer, Heidelberg, **1999**, p. 183; c) T. Ohkuma, R. Noyori in *Comprehensive Asymmetric Catalysis, Vol. I* (Eds.: E. N. Jacobsen, A. Pfaltz, H. Yamamoto), Springer, Heidelberg, **1999**, p. 199; d) H.-U. Blaser, F. Spindler in *Comprehensive Asymmetric Catalysis, Vol. I* (Eds.: E. N. Jacobsen, A. Pfaltz, H. Yamamoto), Springer, Heidelberg, **1999**, p. 247; e) R. Noyori, *Angew. Chem.* **2002**, *114*, 2108; *Angew. Chem. Int. Ed.* **2002**, *41*, 2008; f) W. S. Knowles, *Angew. Chem.* **2002**, *114*, 2096; *Angew. Chem. Int. Ed.* **2002**, *41*, 1998; g) W. Tang, X. Zhang, *Chem. Rev.* **2003**, *103*, 3029; h) I. D. Gridnev, T. Imamoto, *Acc. Chem. Res.* **2004**, *37*, 633; i) X. Cui, K. Burgess, *Chem. Rev.* **2005**, *105*, 3272; j) W. S. Knowles, R. Noyori, *Acc. Chem. Res.* **2007**, *40*, 1238; k) A. J. Minnaard, B. L. Feringa, L. Lefort, J. G. de Vries, *Acc. Chem. Res.* **2007**, *40*, 1267; l) W. Zhang, Y. Chi, X. Zhang, *Acc. Chem. Res.* **2007**, *40*, 1278; m) *Phosphorus Ligands in Asymmetric Catalysis, Vol. I–III* (Ed.: A. Börner), Wiley-VCH, Weinheim, **2008**.

[3] R. A. Sheldon, I. Arends, U. Hanefeld, *Green Chemistry and Catalysis*, Wiley-VCH, Weinheim, **2007**.

[4] a) *Asymmetric Catalysis on Industrial Scale: Challenges, Approaches and Solutions* (Eds.: H. U. Blaser and E. Schmidt), Wiley VCH, Weinheim, **2004**; b) H.-U. Blaser, B. Pugin, F. Spindler, M. Thommen, *Acc. Chem. Res.* **2007**, *40*, 1240.

[5] a) S. Dahmen, S. Brase, *Synthesis* **2001**, 1431; b) A. Hagemeyer, B. Jandeleit, Y. Liu, D. M. Poojary, H. W. Turner, A. F. Volpe, W. Henry Weinberg, *Appl. Catal. A* **2001**, *221*, 23; c) M. T. Reetz, *Angew. Chem.* **2001**, *113*, 292; *Angew. Chem. Int. Ed.* **2001**, *40*, 284; d) J. G. de Vries, A. H. M. de Vries, *Eur. J. Org. Chem.* **2003**, 799; e) C. Gennari, U. Piarulli, *Chem. Rev.* **2003**, *103*, 3071; f) K. Ding, H. Du, Y. Yuan, J. Long, *Chem. Eur. J.* **2004**, *10*, 2872; g) C. Jäkel, R. Paciello, *Chem. Rev.* **2006**, *106*, 2912; h) P. E. Goudriaan, P. W. N. M. van Leeuwen, M.-N. Birkholz, J. N. H. Reek, *Eur. J. Inorg. Chem.* **2008**, 2939.

[6] a) R. Hoen, J. A. F. Boogers, H. Bernsmann, A. J. Minnaard, A. Meetsma, T. D. Tiemersma-Wegman, A. H. M. de Vries, J. G. de Vries, B. L. Feringa, *Angew. Chem.* **2005**, *117*, 4281; *Angew. Chem. Int. Ed.* **2005**, *44*, 4209; b) C. Monti, C. Gennari, U. Piarulli, J. G. de Vries, A. H. M. de Vries, L. Lefort, *Chem. Eur. J.* **2005**, *11*, 6701; c) M. T. Reetz, X. Li, *Angew. Chem.* **2005**, *117*, 3019; *Angew. Chem. Int. Ed.* **2005**, *44*, 2959; d) J. G. de Vries, L. Lefort, *Chem. Eur. J.* **2006**, *12*, 4722.

[7] a) B. Breit, *Angew. Chem.* **2005**, *117*, 6976; *Angew. Chem. Int. Ed.* **2005**, *44*, 6816; b) M. Weis, C. Waloch, W. Seiche, B. Breit, *J. Am. Chem. Soc.* **2006**, *128*, 4188; c) X.-B. Jiang, L. Lefort, P. E. Goudriaan, A. H. M. de Vries, P. W. N. M. van Leeuwen, J. G. de Vries, J. N. H. Reek, *Angew. Chem.* **2006**, *118*, 1245; *Angew. Chem. Int. Ed.* **2006**, *45*, 1223; d) A. J. Sandee, A. M. Van der Burg, J. N. H. Reek, *Chem. Commun.* **2007**, 864; e) G. Hattori, T. Hori, Y. Miyake, Y. Nishibayashi, *J. Am. Chem. Soc.* **2007**, *129*, 12930.

[8] a) A. Vidal-Ferran, A. Moyano, M. A. Pericas, A. Riera, *J. Org. Chem.* **1997**, *62*, 4970; b) A. Vidal-Ferran, N. Bampos, A. Moyano,

M. A. Pericas, A. Riera, J. K. M. Sanders, *J. Org. Chem.* **1998**, *63*, 6309; c) C. Jimeno, A. Vidal-Ferran, A. Moyano, M. A. Pericas, A. Riera, *Tetrahedron Lett.* **1999**, *40*, 777; d) C. Puigjaner, A. Vidal-Ferran, A. Moyano, M. A. Pericas, A. Riera, *J. Org. Chem.* **1999**, *64*, 7902; e) M. A. Pericàs, C. Puigjaner, A. Riera, A. Vidal-Ferran, M. Gomez, F. Jimenez, G. Muller, M. Rocamora, *Chem. Eur. J.* **2002**, *8*, 4164; f) D. Popa, C. Puigjaner, M. Gomez, J. Benet-Buchholz, A. Vidal-Ferran, M. A. Pericas, *Adv. Synth. Catal.* **2007**, *349*, 2265; g) D. Popa, R. Marcos, S. Sayalero, A. Vidal-Ferran, M. A. Pericas, *Adv. Synth. Catal.* **2009**, *351*, 1539.

[9] H. Fernández-Pérez, M. A. Pericas, A. Vidal-Ferran, *Adv. Synth. Catal.* **2008**, *350*, 1984.

[10] a) B. M. Trost, D. L. Van Vranken, C. Bingel, *J. Am. Chem. Soc.* **1992**, *114*, 9327; b) T. V. Rajanbabu, A. L. Casalnuovo, T. A. Ayers, *Adv. Catal. Processes* **1997**, *2*, 1; c) R. Kranich, K. Eis, O. Geis, S. Muhle, J. W. Bats, H.-G. Schmalz, *Chem. Eur. J.* **2000**, *6*, 2874; d) S. J. Degrado, H. Mizutani, A. H. Hoveyda, *J. Am. Chem. Soc.* **2001**, *123*, 755; e) O. Pàmies, G. P. F. van Strijdonck, M. Dieguez, S. Deerenberg, G. Net, A. Ruiz, C. Claver, P. C. J. Kamer, P. W. N. M. van Leeuwen, *J. Org. Chem.* **2001**, *66*, 8867; f) P. I. Dalko, L. Moisan, J. Cossy, *Angew. Chem.* **2002**, *114*, 647; *Angew. Chem. Int. Ed.* **2002**, *41*, 625; g) M. Locatelli, P. G. Cozzi, *Angew. Chem.* **2003**, *115*, 5078; *Angew. Chem. Int. Ed.* **2003**, *42*, 4928; h) J. F. Jensen, I. Sotofte, H. O. Sorensen, M. Johannsen, *J. Org. Chem.* **2003**, *68*, 1258; i) S. Jeulin, S. D. De Paule, V. Ratovelomanana-Vidal, J.-P. Genet, N. Champion, P. Dellis, *Proc. Natl. Acad. Sci. USA* **2004**, *101*, 5799; j) B. Goldfuss, T. Loeschmann, F. Rominger, *Chem. Eur. J.* **2004**, *10*, 5422; k) T. F. Knöpfel, P. Zarotti, T. Ichikawa, E. M. Carreira, *J. Am. Chem. Soc.* **2005**, *127*, 9682; l) J. J. Miller, M. S. Sigman, *J. Am. Chem. Soc.* **2007**, *129*, 2752.

[11] a) N. Sakai, S. Mano, K. Nozaki, H. Takaya, *J. Am. Chem. Soc.* **1993**, *115*, 7033; b) M. J. Baker, P. G. Pringle, *J. Chem. Soc. Chem. Commun.* **1993**, 314.

[12] a) A. Börner, R. Kadyrov, M. Michalik, D. Heller, *J. Organomet. Chem.* **1994**, *470*, 237; b) T. Higashizima, N. Sakai, K. Nozaki, H. Takaya, *Tetrahedron Lett.* **1994**, *35*, 2023; c) A. Kless, J. Holz, D. Heller, R. Kadyrov, R. Selke, C. Fischer, A. Boerner, *Tetrahedron: Asymmetry* **1996**, *7*, 33; d) K. Nozaki, H. Kumobayashi, T. Horiuchi, H. Takaya, T. Saito, A. Yoshida, K. Matsumura, Y. Kato, T. Imai, T. Miura, *J. Org. Chem.* **1996**, *61*, 7658; e) J. Scherer, G. Huttner, M. Buechner, J. Bakos, *J. Organomet. Chem.* **1996**, *520*, 45; f) T. Horiuchi, T. Ohta, E. Shirakawa, K. Nozaki, H. Takaya, *J. Org. Chem.* **1997**, *62*, 4285; g) K. Nozaki, W.-g. Li, T. Horiuchi, H. Takaya, *Tetrahedron Lett.* **1997**, *38*, 4611; h) K. Nozaki, N. Sakai, T. Nanno, T. Higashijima, S. Mano, T. Horiuchi, H. Takaya, *J. Am. Chem. Soc.* **1997**, *119*, 4413; i) K. Nozaki, N. Sato, Y. Tonomura, M. Yasutomi, H. Takaya, T. Hiyama, T. Matsubara, N. Koga, *J. Am. Chem. Soc.* **1997**, *119*, 12779; j) K. Nozaki, Y. Itoi, F. Shibahara, E. Shirakawa, T. Ohta, H. Takaya, T. Hiyama, *J. Am. Chem. Soc.* **1998**, *120*, 4051; k) M. Beller, B. Zimmermann, H. Geissler, *Chem. Eur. J.* **1999**, *5*, 1301; l) K. Nozaki, F. Shibahara, Y. Itoi, E. Shirakawa, T. Ohta, H. Takaya, T. Hiyama, *Bull. Chem. Soc. Jpn.* **1999**, *72*, 1911; m) C. G. Arena, F. Drommi, F. Faraone, *Tetrahedron: Asymmetry* **2000**, *11*, 2765; n) S. Deerenberg, H. S. Schrekker, G. P. F. Van Strijdonck, P. C. J. Kamer, P. W. N. M. Van Leeuwen, J. Fraanje, K. Goubitz, *J. Org. Chem.* **2000**, *65*, 4810; o) S. Deerenberg, P. C. J. Kamer, P. W. N. M. Van Leeuwen, *Organometallics* **2000**, *19*, 2065; p) S. Deerenberg, O. Pamies, M. Dieguez, C. Claver, P. C. J. Kamer, P. W. N. M. van Leeuwen, *J. Org. Chem.* **2001**, *66*, 7626; q) O. Pamies, M. Dieguez, G. Net, A. Ruiz, C. Claver, *J. Org. Chem.* **2001**, *66*, 8364; r) V. Beghetto, A. Scrivanti, U. Matteoli, *Catal. Commun.* **2001**, *2*, 139; s) D. Bonafoux, Z. Hua, B. Wang, I. Ojima, *J. Fluorine Chem.* **2001**, *112*, 101.

[13] a) G. Franciò, K. Wittmann, W. Leitner, *J. Organomet. Chem.* **2001**, *621*, 130; b) K. Nozaki, T. Matsuo, F. Shibahara, T. Hiyama, *Adv. Synth. Catal.* **2001**, *343*, 61; c) A. Suárez, A. Pizzano, *Tetrahedron: Asymmetry* **2001**, *12*, 2501; d) F. Blume, S. Zemolka, T. Fey, R. Kranich, H.-G. Schmalz, *Adv. Synth. Catal.* **2002**, *344*, 868; e) A. Suarez, M. A. Mendez-Rojas, A. Pizzano, *Organometallics* **2002**, *21*, 4611;

f) F. Shibahara, K. Nozaki, T. Hiyama, *J. Am. Chem. Soc.* **2003**, *125*, 8555; g) C. J. Cobley, K. Gardner, J. Klosin, C. Praquin, C. Hill, G. T. Whiteker, A. Zanotti-Gerosa, J. L. Petersen, K. A. Abboud, *J. Org. Chem.* **2004**, *69*, 4031; h) X. Jia, X. Li, W. S. Lam, S. H. L. Kok, L. Xu, G. Lu, C.-H. Yeung, A. S. C. Chan, *Tetrahedron: Asymmetry* **2004**, *15*, 2273; i) Y. Yan, Y. Chi, X. Zhang, *Tetrahedron: Asymmetry* **2004**, *15*, 2173; j) M. Rubio, A. Suarez, E. Alvarez, A. Pizzano, *Chem. Commun.* **2005**, 628; k) S. Vargas, M. Rubio, A. Suarez, A. Pizzano, *Tetrahedron Lett.* **2005**, *46*, 2049; l) B. Breit, E. Fuchs, *Synthesis* **2006**, 2121; m) C. Müller, L. G. Lopez, H. Kooijman, A. L. Spek, D. Vogt, *Tetrahedron Lett.* **2006**, *47*, 2017; n) S. Vargas, M. Rubio, A. Suarez, A. Pizzano, *Tetrahedron Lett.* **2006**, *47*, 615; o) S. Vargas, M. Rubio, A. Suarez, D. Del Rio, E. Alvarez, A. Pizzano, *Organometallics* **2006**, *25*, 961; p) K. Burgemeister, G. Francio, V. H. Gego, L. Greiner, H. Hugl, W. Leitner, *Chem. Eur. J.* **2007**, *13*, 2798; q) M. Rubio, S. Vargas, A. Suarez, E. Alvarez, A. Pizzano, *Chem. Eur. J.* **2007**, *13*, 1821; r) T. Robert, J. Velder, H.-G. Schmalz, *Angew. Chem.* **2008**, *120*, 7832; *Angew. Chem. Int. Ed.* **2008**, *47*, 7718; s) J. Velder, T. Robert, I. Weidner, J.-M. Neudoerfl, J. Lex, H.-G. Schmalz, *Adv. Synth. Catal.* **2008**, *350*, 1309.

[14] a) A. Vidal-Ferran, A. Moyano, M. A. Pericas, A. Riera, *Tetrahedron Lett.* **1997**, *38*, 8773; b) J. Rudolph, C. Bolm, P.-O. Norrby, *J. Am. Chem. Soc.* **2005**, *127*, 1548; c) D. Balcells, F. Maseras, G. Ujaque, *J. Am. Chem. Soc.* **2005**, *127*, 3624; d) E. Zuidema, L. Escorihuela, T. Eichelsheim, J. J. Carbo, C. Bo, P. C. J. Kamer, P. W. N. M. van Leeuwen, *Chem. Eur. J.* **2008**, *14*, 1843.

[15] a) D. Balcells, F. Maseras, *New J. Chem.* **2007**, *31*, 333; b) J. M. Brown, R. J. Deeth, *Angew. Chem.* **2009**, *121*, 4544; *Angew. Chem. Int. Ed.* **2009**, *48*, 4476.

[16] a) J. Halpern, D. P. Riley, A. S. C. Chan, J. J. Pluth, *J. Am. Chem. Soc.* **1977**, *99*, 8055; b) A. S. C. Chan, J. J. Pluth, J. Halpern, *J. Am. Chem. Soc.* **1980**, *102*, 5952; c) R. Wilczynski, W. A. Fordyce, J. Halpern, *J. Am. Chem. Soc.* **1983**, *105*, 2066; d) C. R. Landis, J. Halpern, *J. Am. Chem. Soc.* **1987**, *109*, 1746.

[17] J. M. Brown, *Chem. Soc. Rev.* **1993**, *22*, 25.

[18] a) C. R. Landis, P. Hilfenaus, S. Feldgus, *J. Am. Chem. Soc.* **1999**, *121*, 8741; b) S. Feldgus, C. R. Landis, *J. Am. Chem. Soc.* **2000**, *122*, 12714; c) C. R. Landis, S. Feldgus, *Angew. Chem.* **2000**, *112*, 2985; *Angew. Chem. Int. Ed.* **2000**, *39*, 2863; d) S. Feldgus, C. R. Landis, *Organometallics* **2001**, *20*, 2374.

[19] S. Mori, T. Vreven, K. Morokuma, *Chem. Asian J.* **2006**, *1*, 391.

[20] a) P. J. Donoghue, P. Helquist, P. O. Norrby, O. Wiest, *J. Chem. Theory Comput.* **2008**, *4*, 1313; b) P. J. Donoghue, P. Helquist, P. O. Norrby, O. Wiest, *J. Am. Chem. Soc.* **2009**, *131*, 410.

[21] a) D. A. Evans, F. E. Michael, J. S. Tedrow, K. R. Campos, *J. Am. Chem. Soc.* **2003**, *125*, 3534; b) H.-J. Drexler, W. Baumann, T. Schmidt, S. Zhang, A. Sun, A. Spannenberg, C. Fischer, H. Buschmann, D. Heller, *Angew. Chem.* **2005**, *117*, 1208; *Angew. Chem. Int. Ed.* **2005**, *44*, 1184.

[22] M. T. Reetz, A. Meiswinkel, G. Mehler, K. Angermund, M. Graf, W. Thiel, R. Mynott, D. G. Blackmond, *J. Am. Chem. Soc.* **2005**, *127*, 10305.

[23] I. D. Gridnev, C. Fan, P. G. Pringle, *Chem. Commun.* **2007**, 1319.

[24] W. S. Knowles, *Acc. Chem. Res.* **1983**, *16*, 106.

[25] CCDC-752670 (**5 e**), 752671 (**5 f**), 752672 (**9**), and 752673 (**10**) contain the supplementary crystallographic data for the structures reported in this paper. These data can be obtained free of charge from The Cambridge Crystallographic Data Centre via www.ccdc.cam.ac.uk/data_request/cif.

[26] The steric environment at this position has proved to be critical in the catalytic activity of other chiral ligands derived from Sharpless epoxy alcohols in several asymmetric transformations. See reference [8] and C. Jimeno, A. Vidal-Ferran, M. A. Pericas, *Org. Lett.* **2006**, *8*, 3895.

[27] Compound **7h** was obtained in 55 % yield and 80 % purity. Attempts to further purify it led to product decomposition. However, these impurities did not interfere in the preparation of [Rh(nbd)(**7h**)]BF₄, which was obtained as a pure compound.

[28] See the Supporting Information for details.

[29] Methyl *N*-acetylaminoacrylate (**16b**) was studied together with **13** as test substrate. The same trends observed for **13** were also observed for **16b**. See the Supporting Information for details.

[30] Analogously, **8b** should be regarded as the mismatched combination.

[31] Compound **15** could be easily synthesized by *O*-phosphorylation of commercially available 2-(diphenylphosphino)ethanol with the chlorophosphite derived from (*S*)-BINOL (see the Experimental Section in the Supporting Information) under basic conditions.

[32] H.-J. Drexler, W. Baumann, A. Spannenberg, C. Fischer, D. Heller, *J. Organomet. Chem.* **2001**, *621*, 89.

[33] J. Bayardon, J. Holz, B. Schaeffner, V. Andrushko, S. Verevkin, A. Preetz, A. Boerner, *Angew. Chem.* **2007**, *119*, 6075; *Angew. Chem. Int. Ed.* **2007**, *46*, 5971.

[34] Hydrogenation of dehydroamino acids with conventional N-protecting groups (Boc and Cbz) has not been so widely studied as the N-acyl derivatives. See, for example, references [21a], [45], and the following: a) N. W. Boaz, E. B. Mackenzie, S. D. Debenham, S. E. Large, J. A. Ponasik, Jr., *J. Org. Chem.* **2005**, *70*, 1872 and b) X. Han, X.-J. Jiang, R. L. Civiello, A. P. Degnan, P. V. Chaturvedula, J. E. Macor, G. M. Dubowchik, *J. Org. Chem.* **2009**, *74*, 3993.

[35] a) G. Zhu, X. Zhang, *J. Org. Chem.* **1998**, *63*, 3133; b) G. Zhu, P. Cao, Q. Jiang, X. Zhang, *J. Am. Chem. Soc.* **1997**, *119*, 1799.

[36] T. Kuroita, T. Oda, Y. Asano, N. Taya, K. Iwanaga, H. Tokuhara, Y. Fukase (Takeda Pharmaceutical Company), WO 139941, **2008**; [*Chem. Abstr.* **2009**, *150*, 5764].

[37] To the best of our knowledge, asymmetric hydrogenation of cyclic enamides has not been efficiently mediated by very many catalytic systems. See, for example: a) M. J. Burk, G. Casy, N. B. Johnson, *J. Org. Chem.* **1998**, *63*, 6084; b) Z. Zhang, G. Zhu, Q. Jiang, D. Xiao, X. Zhang, *J. Org. Chem.* **1999**, *64*, 1774; c) W. Tang, Y. Chi, X. Zhang, *Org. Lett.* **2002**, *4*, 1695; d) H. Bernsmann, M. van den Berg, R. Hoen, A. J. Minnaard, G. Mehler, M. T. Reetz, J. G. de Vries, B. L. Feringa, *J. Org. Chem.* **2005**, *70*, 943; e) F. W. Patureau, S. de Boer, M. Kuil, J. Meeuwissen, P.-A. R. Breuil, M. A. Siegler, A. L. Spek, A. J. Sandee, B. de Bruin, J. N. H. Reek, *J. Am. Chem. Soc.* **2009**, *131*, 6683.

[38] a) M. Sawamura, R. Kuwano, Y. Ito, *J. Am. Chem. Soc.* **1995**, *117*, 9602; b) C. Pautigny, S. Jeulin, T. Ayad, Z. Zhang, J.-P. Genet, V. Ratovelomanana-Vidal, *Adv. Synth. Catal.* **2008**, *350*, 2525; c) J. Wassenaar, M. Kuil, J. N. H. Reek, *Adv. Synth. Catal.* **2008**, *350*, 1610.

[39] Hydrogenation was conducted at 0 °C to increase enantioselectivity. When the reaction was performed at room temperature, the enantiomeric excess was lower (90 % *ee*).

[40] H. B. Kagan, P. Dang Tuan, *J. Am. Chem. Soc.* **1972**, *94*, 6429.

[41] B. D. Vineyard, W. S. Knowles, M. J. Sabacky, G. L. Bachman, D. J. Weinkauff, *J. Am. Chem. Soc.* **1977**, *99*, 5946.

[42] A. Togni, C. Breutel, A. Schnyder, F. Spindler, H. Landert, A. Tijani, *J. Am. Chem. Soc.* **1994**, *116*, 4062.

[43] A. Miyashita, A. Yasuda, H. Takaya, K. Toriumi, T. Ito, T. Souchi, R. Noyori, *J. Am. Chem. Soc.* **1980**, *102*, 7932.

[44] I. D. Gridnev, T. Imamoto, G. Hoge, M. Kouchi, H. Takahashi, *J. Am. Chem. Soc.* **2008**, *130*, 2560.

[45] Present work.

[46] H. J. Kreuzfeld, C. Doebler, H. W. Krause, C. Facklam, *Tetrahedron: Asymmetry* **1993**, *4*, 2047.

[47] M. J. Burk, *J. Am. Chem. Soc.* **1991**, *113*, 8518.

[48] J. M. Hopkins, S. A. Dalrymple, M. Parvez, B. A. Keay, *Org. Lett.* **2005**, *7*, 3765.

[49] J. You, H.-J. Drexler, S. Zhang, C. Fischer, D. Heller, *Angew. Chem.* **2003**, *115*, 942; *Angew. Chem. Int. Ed.* **2003**, *42*, 913.

[50] Y.-Y. Yan, T. V. RajanBabu, *Org. Lett.* **2000**, *2*, 199.

[51] M. J. Burk, Y. M. Wang, J. R. Lee, *J. Am. Chem. Soc.* **1996**, *118*, 5142.

[52] T. Sento, S. Shimazu, N. Ichikun, T. Uematsu, *J. Mol. Catal. A* **1999**, *137*, 263.

[53] W. C. Christopfel, B. D. Vineyard, *J. Am. Chem. Soc.* **1979**, *101*, 4406.

[54] M. J. Burk, F. Bienewald, M. Harris, A. Zanotti-Gerosa, *Angew. Chem.* **1998**, *110*, 2034; *Angew. Chem. Int. Ed.* **1998**, *37*, 1931.

[55] P. M. Donate, D. Frederico, R. da Silva, M. G. Constantino, G. Del Ponte, P. S. Bonatto, *Tetrahedron: Asymmetry* **2003**, *14*, 3253.

[56] For previous computational studies on asymmetric hydrogenation with $C_2$ symmetric ligands, see: a) references [18–20], b) M. Li, D. Tang, X. Luo, W. Shen, *Int. J. Quantum Chem.* **2005**, *102*, 53. For previous computational studies with $C_1$-symmetric ligands see reference [23b].

[57] S. M. A. Donald, A. Vidal-Ferran, F. Maseras, *Can. J. Chem.* **2009**, *87*, 1273.

[58] A. R. Rossi, R. Hoffmann, *Inorg. Chem.* **1975**, *14*, 365.